RSC Advances

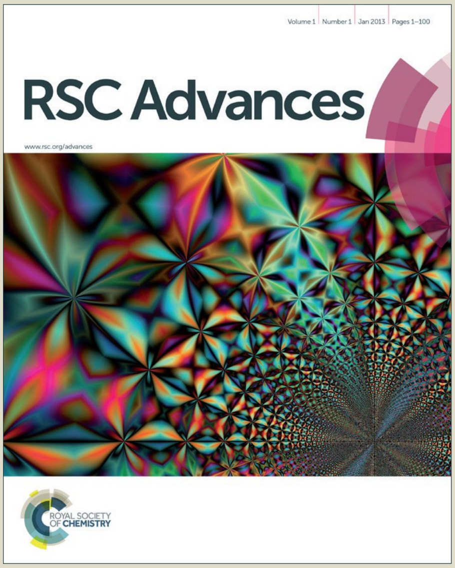

ROYAL SOCIETY OF CHEMISTRY

www.rsc.org/advances

Mechanisms and Kinetic Parameters for the Gas-phase Reactions of Anthracene and Pyrene with Cl Atoms in the Presence of NOx

Juan Dang, Maoxia He*

Environment Research Institute, Shandong University，

Jinan 250100, P. R. China

---

*Corresponding author. E-mail: hemaox@sdu.edu.cn

Fax: 86-531-8836 1990

Abstract

Due to the global dispersion and toxicities, polycyclic aromatic hydrocarbons (PAHs) in the atmosphere have become a serious environmental concern. Atmospheric reactions of PAHs with Cl atoms may be of critical importance in specific areas such as the marine boundary layer and coastal regions. In this work, the mechanisms of the Cl radical-initiated atmospheric oxidation of anthracene (Ant) and pyrene (Pyr) were investigated by using quantum chemistry calculations. The rate constants for the crucial elementary reactions were estimated. The oxidation products of the gas-phase reactions of Ant and Pyr with Cl atoms are chloro-Ants, chloro-Pyrs, 2-chloroanthracen-1-one, 1-chloropyren-2-one, 1-chloropyren-3-one, 4-chloropyren-5-one, 1-chloro-2-hydroperoxyanthracene, 2-chloro-1-hydroperoxyanthracene, 1-chloro-2-hydroperoxypyrene, 4-chloro-5-hydroperoxypyrene, epoxides, dialdehydes, 9-nitroanthracene, 1-nitroanthracene and nitropyrenes. 9-nitroanthracene can be easier produced by the gas-phase reaction of Ant with Cl atoms than that of Ant with OH radicals. water plays a vital role in the formation of 9-nitroanthracene resulting from the reactions with NO_2. This comprehensive mechanism study is the first one reported for the Cl radical-initiated atmospheric oxidation of PAHs. The calculated overall rate constants for the Cl addition reactions of Ant and Pyr are 5.87×10^{-12} and 2.81×10^{-12} cm^3 $molecule^{-1}$ s^{-1} at 298 K and 1 atm, respectively.

Keywords: Anthracene, Pyrene, Cl atoms, Oxidation mechanisms, Degradation products, Rate constants

1. Introduction

Polycyclic aromatic hydrocarbons (PAHs) are a class of ubiquitous environmental contaminants that mainly arise from incomplete combustion of fossil fuels and biomass.[1-3] PAHs have been constantly detected in the atmosphere throughout the world.[4-7] The annual atmospheric emissions of 16 priority PAHs in Asian countries accounted for 53.5% of the total global emissions (504 Gg), with the highest emission from China (106 Gg) and India (67 Gg) in 2007.[8] Because of their prevalent occurrence, persistence in the environmental matrices and extremely hazardous properties to human health,[9-11] the fate of these compounds in the atmosphere is of high public concern.

In the troposphere, PAHs can undergo gas-phase reactions with OH radical, NO_3 radical, O_3 and chlorine atom.[12, 13] Although the reactions with OH radical, NO_3 radical, O_3 are generally considered to be the main sinks for gaseous PAHs, the reactions with Cl atom may be significant in the marine boundary layer and in coastal regions, especially in the Arctic lower troposphere during spring.[12-14] The peak concentration of Cl atoms is up to 10^5 molecule cm^{-3} or more in the marine boundary layer at dawn.[13,15,16] In addition, chlorine atoms are highly reactive towards organic substances, which are 10^3 times more reactive than OH radicals.[17] Hence even at relatively low concentrations, chlorine atoms have the ability to enhance organics oxidation in the atmosphere. Previous studies showed that the rate constants for the reactions of many volatile organic compounds with Cl atoms are ~10^2 higher than those for reactions with OH radicals.[13] Therefore the Cl atom reactions could play an important role in the atmospheric oxidation of PAHs in specific areas such as the marine boundary layer and coastal regions. In particular, some oxidation products (chlorinated PAHs included) of atmospheric reactions of PAHs with Cl atoms have been identified enhanced toxicities, mutagenicities and aryl hydrocarbon receptor activities compared with the corresponding parent PAHs.[18-20] Hence, it is necessary to investigate the reaction mechanisms of PAHs with Cl atoms to clarify their atmospheric transformations. To date, only two studies (Wang et al, 2005 and Long et al, 2007) reported the rate constants for the reactions of naphthalene and alkylnaphthalenes with Cl atoms, and the reaction mechanisms have not been fully elucidated.[13, 21,22] Clearly, more work is needed to obtain a comprehensive knowledge.

Anthracene (Ant) and pyrene (Pyr) are members of the 16 USEPA priority PAHs, which have been detected at high concentrations in certain areas.[12,23,24] During the summer of 2003, the field measurements in the Shing Mun Tunnel of Hong Kong showed that the average ambient air concentrations of Ant ranged from 30.5 to 15.0 ng m^{-3}.[23] In 2008, air samples collected from Oporto metropolitan area in northern Portugal revealed that the maximum concentration of Pyr was up to 9.44 ng m^{-3}.[25] Considering their widespread occurrence in air, it is critical to clarify the gas-phase reactions of Ant and Pyr with Cl atoms. Due to the scarcity of efficient detection schemes for intermediate radicals in the experimental studies, quantum chemical calculation can be of considerable help to illuminate the reaction mechanisms. In this work, we carried out a theoretical study on the Cl-initiated atmospheric oxidation of Ant and Pyr in the presence of NO_x by using density functional theory (DFT).[26] Modeling of the fate of PAHs in the atmosphere places a high demand on kinetic parameters. Therefore the rate constants of key elementary reactions involved in the Cl-initiated oxidation of Ant and Pyr were also calculated.

2. Computational Method

The quantum chemical calculations were performed with the Gaussian 09 software package[27] on a supercomputer. The geometries of the reactants, intermediates, transition states and products were optimized at the BB1K/6-31+G(d,p) level. The vibrational frequencies were calculated to identify the structures obtained as true minima or first-order saddle points. The intrinsic reaction coordinate (IRC) analysis was carried out to confirm that each transition state connects to the right minima along the reaction path. A more flexible basis set, 6-311+G(3df,2p), was used to determine the single point energies of various species. The overall energetic profiles were constructed to locate the energetically favorable reaction pathways.

The MESMER program, a Master Equation Solver for Multi-Energy Well Reactions, which uses matrix techniques to formulate and solve the energy grained master equation (EGME) for reaction systems composed of an arbitrary number of wells, transition states, sinks, and reactants. The master equation is:[28]

$$\frac{d}{dt}\mathbf{p} = \mathbf{Mp} \qquad (1)$$

Where **p** is the population vector including the populations of the energy grains for each isomer and **M** is the matrix describing population evolution due to collisional energy transfer and reaction.

The grain size used is 100 cm−1, and the maximum grain energy is 25 kT in the calculation process. Classical method is applied to calculate the density of states. The exponential down model was implemented for describing collisional transfer probabilities. SimpleRRKM or the MesmerILT method is provided for the calculation of rate constants.

For reactions with a well-defined transition state, the common way of obtaining rate constants from a particular energy grain, *k*(E), were determined by using Rice-Ramsperger-Kassel-Marcus (RRKM) theory. The RRKM expression is given by: [28]

$$k(E) = \frac{W(E - E_0)}{h\rho(E)} \qquad (2)$$

Where $W(E\text{-}E_0)$ is the rovibrational sum of states at the transition state, E_0 is the reaction threshold energy, $\rho(E)$ is the density of rovibrational states of reactants, and h is Planck’s constant.

If no transition state is specified, an inverse Laplace transform (ILT) provides a mathematical formalism for deriving *k*(E)s from an Arrhenius fit to a set of *k*(*E*)s. The basis of the ILT is the standard Boltzmann average which may be expressed as: [28]

$$k^{\infty}(\beta) = \frac{1}{Q(\beta)} \int_{0}^{\infty} k(E)\rho(E)\exp(-\beta E)dE \tag{3}$$

Where $Q(\beta)$ is the corresponding canonical partition function and $\rho(E)$ is the reactant rovibrational density of states. Then representing $k^{\infty}(\beta)$ by an modified Arrenhius expression can obtain k(E) as an ILT.

3. Results and Discussion

3.1 Reactions with Cl atoms

The atmospheric reactions of volatile organic compounds with Cl atoms proceed via Cl addition to the C=C bonds and H abstraction by Cl atoms. Vereecken et al showed that H abstraction by Cl atoms is less important, even for abstraction of the highly reactive allylic hydrogen atoms.[29] According to our simulation, the H abstraction from Ant and Pyr are endothermic reactions, for example, the H abstractions from position C1, C2, C9 of Ant are endothermic by 7.59 kcal/mol, 7.85 kcal/mol, 8.33 kcal/mol, respectively. However, the Cl addition reactions are highly exothermic. Thus, only the Cl addition reactions were discussed in this paper. For convenience of description, the C atoms in Ant and Pyr are numbered, as presented in Figure 1. The Ant molecule at ground state is of D_{2h} symmetry, C atoms in Ant fall into four groups: C1, C4, C5 and C8 atoms belong to one equivalent group; C2, C3, C6 and C7; C9 and C10; C11, C12, C13 and C14 belong to the other three equivalent groups. Three different Cl-Ant adduct isomers can be formed via Cl addition to C1, C2 and C9 atoms. Particularly, the corresponding Cl-Ant adduct cannot be formed from the Cl addition to C11 position. Analysis of the molecular structure of Pyr shows that there are four different kinds of C atoms theoretically leading to four Cl addition processes. As the Cl addition to C2 and C3a positions cannot occur, only two Cl-Pyr adducts are generated. The reaction schemes of the Cl additions embedded with reaction heats (∆*H*, 0K) are depicted in Figure 1. The configuration of the Cl-Ant adducts and Cl-Pyr adducts (IM1-IM5) are shown in Figure S1 of supporting information.

All of the Cl addition pathways are highly exothermic with no potential barriers, which indicate that they can occur readily under general atmospheric conditions. According to the previous research, there is also no potential barrier on the addition pathway for the reaction of Cl with benzene.[30] At the BB1K/6-311+G(3df,2p) level, the reaction heats of the Cl addition reactions are distributed between -19.83 and -16.31 kcal/mol. The resulting Cl-Ant and Cl-Pyr adducts will further react with O_2/NO_x as their removal.

3.2 Secondary Reactions

3.2.1 Reactions with O_2

Based on the analysis above, the reactions of Ant and Pyr with Cl atoms can readily occur under general atmospheric conditions. The resulting adducts, Cl-Ants and Cl-Pyrs, are important intermediates. In the atmosphere, they can further react with O_2/NO_x as their degradation. As shown in Figure 2, the Cl-Ant and Cl-Pyr adducts can react with O_2 to yield the corresponding monochloro-Ants, monochloro-Pyrs and HO_2. Löfroth et al. found that 9-chloroAnt shows strong direct mutagenic effects.[31] Monochloro-Ants and monochloro-Pyrs can further proceed with Cl atoms addition and H abstraction by O_2 to produce dichloro-Ants and dichloro-Pyrs. The Cl addition reactions are barrierless and exothermic by 7.78~20.29 kcal/mol. It should be noted that the formation of dichloro-Ants is more difficult than the generation of monochloro-Ants, because of the relative higher potential barriers of H abstractions by O_2. To be specific, the potential barriers of these H abstraction processes are 24.44~18.00 kcal/mol at the BB1K/6-311+G(3df,2p) level. Similarly, polychlorinated Ants and polychlorinated Pyrs can be produced by continuous Cl additions and H abstractions. According to the literature, the AhR (aryl hydrocarbon receptor)-mediated toxic activities of chloroanthracenes tend to increase with increasing chlorine substitution.[32]

The reaction of the Cl-Ant and Cl-Pyr adducts with O_2/NO are displayed in Figure 3. O_2 can attack on the C atoms with an unpaired electron in Cl-Ant and Cl-Pyr from two different directions: the *cis* or *trans*-position of the -Cl group with respect to the aromatic ring (Figure S2 of supporting information). Therefore, six O_2-Cl-Ant adducts and four O_2-Cl-Pyr adducts are expected to be formed. By comparison of the potential barriers and reaction heats of these reaction pathways, the O_2 addition from *trans*-position of the -Cl group is favored over those of the other ones. So just the subsequent reactions of the favorable adducts are depicted in Figure 3. As shown, the O_2-Cl-Ant adducts IM10 and IM13 have similar reaction channels, which include barrierless association of NO, rupture of the O-ONO bond, elimination of HCl and H abstraction by O_2. Calculations show that 2-chloroanthracen-1-one and the radical P12 is more easily to be obtained because of the lower potential barrier and strong exothermicity. The intermediate IM16 is difficult to be formed by O_2 addition. The potential barrier of this reaction is calculated to be 65.38 kcal/mol and the process is endothermic by 41.58 kcal/mol. The intermediate IM17 formed by O_2 addition can undergo NO addition without potential barrier, followed by cleavage of the O-ONO bond, H abstraction by O_2 and rupture of the C-O bond, leading to the formation of 1-chloropyren-2-one and 1-chloropyren-3-one. The subsequent reactions of IM22 are similar to those of IM17, resulting in the formation of 4-chloropyren-5-one. The calculated profiles of the potential energy surface show that the reaction of the cleavage of O-ONO bond is the rate-determining process due to its high potential barrier.

As shown in Figure 4, the intermediate IM10 produced by O_2 addition can also proceed with H migration from the C atom to the O atom, leading to the formation of IM25. The subsequent reaction of IM25 involves two elementary reactions: elimination of HO_2 radical and H abstraction by O_2. These processes ultimately result in the generation of 1-chloroanthracene and 1-chloro-2-hydroperoxyanthracene. Through the analysis and comparison, the reaction of the H migration is the rate-determining step due to the high potential barrier. The potential barrier of the H migration is calculated to be 26.50 kcal/mol and the process is exothermic by 3.94 kcal/mol. Similarly, 2-chloroanthracene, 2-chloro-1-hydroperoxyanthracene, 1-chloropyrene, 1-chloro-2-hydroperoxypyrene, 4-chloropyrene, 4-chloro-5-hydroperoxypyrene can be formed by the subsequent reactions of IM13, IM17 and IM22 via an analogous mechanism. The potential barriers of these H migration processes are 28.44~25.26 kcal/mol at the BB1K/6-311+G(3df,2p) level, and the processes are exothermic by 1.60~8.39 kcal/mol.

As presented in Figure 5, the intermediate IM10 undergo intramolecular cyclization to produce bicyclic peroxy radicals (IM29). IM29 can further proceed with O_2 addition, NO barrierless addition and elimination of NO_2, resulting in the formation of the important intermediate IM32. The subsequent reaction of IM32 involves three reaction channels: H abstraction by O_2 and two different ways of synchronous cleavage of the O-O bond and C-C bond. Obviously, compared with the H abstraction, the ring-opening reactions have lower barriers and release more heat. Hence, the ring-opening reactions are the energetically more favorable reaction pathways. These processes ultimately result in the formation of a bridge-ring compound (P21) and two dialdehydes (P22 and P23). The reaction channel of IM13 contains three elementary reactions: ring-closure, cleavage of O-O bond and H abstraction by O_2. These reactions are thermodynamically favorable under general atmospheric conditions and lead to the generation of an epoxide (P24). Similarly, IM17 and IM22 can also proceed with ring-closure, ring-opening and H abstraction by O_2 to yield epoxides (P25 and P27) and phenalenone radical (P26).

3.2.2 Reactions with NO_2

The Cl-Ant and Cl-Pyr adducts (IM1-IM5) also can react with NO_2 to form Cl-NO_2-Ant and Cl-NO_2-Pyr adducts via barrierless associations. These processes are strongly exothermic by 18.89~38.01 kcal/mol. The reaction schemes of NO_2 addition are depicted in Figure 6. The Cl-NO_2-Ant and Cl-NO_2-Pyr adducts (IM40, IM42, IM44, IM45) may subsequently undergo unimolecular decomposition to yield nitro-Ants and nitro-Pyrs via the direct loss of HCl. As shown in Figure 6 (black arrows), the reaction potential barriers of the direct elimination of HCl are relatively high (31.43~41.96 kcal/mol), thus the reactions are difficult to occur under the typical atmospheric environment.

As we all know, water is one of the massive atmospheric constituents and can participate in the reactions through forming hydrogen bonded complexes in the atmosphere.[32] With the participation of water, the eliminations of HCl from the Cl-NO_2-Ant and Cl-NO_2-Pyr adducts can become bimolecular reactions (Cl-NO_2-Ant+H_2O and Cl-NO_2-Pyr+H_2O). A six-membered ring transition state (Figure S3 of supporting information) can be formed, in which the water molecule accepts the hydrogen from the aromatic ring and simultaneously donates another hydrogen atom to the Cl atom. The potential barriers of eliminations of HCl and H_2O via the bimolecular reactions are 7.65~8.59 kcal/mol lower than those of the direct loss of HCl.

Particularly, when Cl atoms add to the C_1 atom of Ant, the corresponding Cl-NO_2-Ant adducts are hybrids of several resonance structures (shown in Figure S4 of supporting information). The unpaired electron can be distributed to the *ortho* and *para* positions of the -Cl group, therefore NO_2 can add to these positions to form the intermediates IM40 and IM41. It was reported that the atmospheric concentration of water dimer is up to 6×10^{14} molecule cm^{-3} at 292 K.[34] As described in Figure 6 (red arrows), with the aid of the water dimer, 1-nitroanthracene and 9-nitroanthracene can be formed from the elimination of HCl and H_2O. The potential barrier of the formation of 1-nitroanthracene is calculated to be 17.37 kcal/mol and the process is exothermic by 15.11 kcal/mol. 9-Nitroanthracene is one of the most abundant nitro-PAHs in the atmosphere. Our previous study confirmed that 9-nitroanthracene can be generated by the OH or NO_3 radical-initiated gas-phase reactions of Ant but not just originate from the primary emissions and heterogeneous reactions.[35] As a supplement to our previous work, 9-nitroanthracene also can be produced by the gas-phase reactions of Ant with Cl atoms. Compared with our previous researches, the formation of nitroanthracenes and nitropyrenes from the Cl-initiated gas-phase reactions are easier than from the reactions of Ant and Pyr with OH radicals because of the relatively lower barriers.[35] For instance, the potential barrier of the formation of 9-nitroanthracene from the OH-initiated reactions of Ant is 30.75 kcal/mol,[35] and the barrier of the corresponding reaction of Ant with OH radicals is 24.97 kcal/mol.

3.3 Rate Constant Calculations

For clarifying the atmospheric fates of Ant and Pyr, it is essential to determine accurate rate constants of the elementary reactions involved in the

Cl-initiated atmospheric oxidations of Ant and Pyr. On the basis of the BB1K/6-311+G(3df,2p)//BB1K/6-31+G(d,p) energies, the rate constants of the key elementary reactions involved in the Cl-initiated oxidation of Ant and Pyr were evaluated at 298 K and 1 atm by using MESMER, which has been successfully applied in the calculation of several similar reactions.[28,36] The calculated rate constants of the crucial elementary reactions are organized in Table 1. The individual rate constants for the Cl additions to the C_1-H, C_2-H and C_3-H bonds of Ant are noted as k_1, k_2, k_3, respectively. Similarly, the rate constants of the Cl additions to the C_1-H and C_3-H bonds of Pyr are denoted as k_4, k_5, respectively. Considering the molecular symmetries of Ant and Pyr, the overall rate constants for the Cl addition reactions of Ant and Pyr are depicted as k_a and k_p, $k_a=(k_1+k_2)\times4+k_3\times2$ and $k_a=(k_4+k_5)\times4$, respectively. The calculated overall rate constants of Ant and Pyr (k_a and k_p) are 5.87×10^{-12} and 2.81×10^{-12} cm^3 molecule^{-1} s^{-1} at 298 K and 1 atm, respectively. Due to the absence of the available experimental information, it is difficult to make a direct comparison of the calculated rate constants with the experimental values for the reactions of Ant and Pyr with Cl atoms. According to the literature, the rate constant for the gas-phase reaction of naphthalene with Cl atoms is $\leqq 0.0091\pm0.0003\times10^{-10}$ cm^3 molecule^{-1} s^{-1} at 296 K and 735 Torr.[13] The calculated rate constants for the reactions of Ant and Pyr with Cl atoms are relatively consistent with the published experimental value of naphthalene. The rate constants of the elementary reactions listed in Table 1 can be of help for the construction of detailed kinetic models describing the atmospheric fates of Ant and Pyr.

Based on the overall rate constants for the reactions of Ant and Pyr with Cl atoms (k_a and k_p) and a detected Cl concentration (C_{cl}) of 4.0×10^5 molecule cm^{-3} in the marine boundary layer,[37] from the expressions:

$$\tau = \frac{1}{k \times c_{\mathrm{Cl}}} \qquad (k=k_a \text{ or } k_p)$$

The atmospheric lifetimes (τ) of Ant and Pyr determined by Cl atoms are calculated to be 4.93 and 7.27 days, respectively.

4. Conclusions and Environmental Implications

This work presented a comprehensive theoretical study on the reaction mechanisms of the Cl atom-initiated atmospheric oxidations of Ant and Pyr. The individual rate constants were determined. Several conclusions can be drawn from this study:

(1) All of the Cl addition pathways are highly exothermic with no potential barriers, and they can readily occur under general atmospheric conditions.

(2) The products of the Cl atom-initiated atmospheric oxidations of Ant and Pyr include monochloro-Ants, monochloro-Pyrs, dichloro-Ants, dichloro-Pyrs, 2-chloroanthracen-1-one, 1-chloropyren-2-one, 1-chloropyren-3-one, 4-chloropyren-5-one, 1-chloro-2-hydroperoxyanthracene, 2-chloro-1-hydroperoxyanthracene, 1-chloro-2-hydroperoxypyrene, 4-chloro-5-hydroperoxypyrene, epoxides, dialdehydes, 9-nitroanthracene,

1-nitroanthracene and nitropyrenes. Particularly, water plays a crucial role in the gas-phase formation of 9-nitroanthracene, which can be easier formed by the gas-phase reaction of Ant with Cl atoms than that of Ant with OH radicals.

(3) The calculated overall rate constants of Ant and Pyr (k_a and k_p) are 5.87×10^{-12} and 2.81×10^{-12} cm^3 $molecule^{-1}$ s^{-1} at 298 K and 1 atm, respectively. In the marine boundary layer, the atmospheric lifetimes of Ant and Pyr determined by Cl atoms are calculated to be 4.93 and 7.27 days, respectively.

In the troposphere, Ant and Pyr can be transformed by the chemical processes of reactions with the OH radical during the daytime, reactions with NO_3 radical during evening and nighttime, and reactions with Cl atoms in coastal areas. According to the literature, reactions of Ant and Pyr with O_3 can be of negligible importance in the atmosphere due to slow reactions with the aromatic ring.[12] The lifetime for Ant and Pyr determined by reactions with OH is about 2-6 hours,[12] which is much shorter than that of reaction with Cl atoms in the atmosphere. Although the reaction with OH radical plays the most important role in the atmospheric oxidations of Ant and Pyr, it is also necessary to understand the reaction with Cl due to the high concentration of Cl atoms in the marine boundary layer and in coastal regions. Besides, the formation pathway of chlorinated PAHs (more dangerous compounds) in the atmosphere can be obtained from the reaction with Cl atoms. The simulated results need more experimental data to prove it. In order to clarify the potential risk thoroughly, it deserves further studies with the combination of experimental and the theoretical analyses.

Acknowledgment

The work was financially supported by NSFC (National Natural Science Foundation of China, project Nos. 21337001, 21377073).

Supporting Information Available

Configuration of the Cl-Ant adducts and Cl-Pyr adducts (IM1-IM5). The O_2 addition reaction schemes of Ant and Pyr embedded with the potential barrier ΔE (kcal/mol) and reaction heat ΔH (kcal/mol). Configuration of the transition states for the elimination of water and HCl from the Cl-NO_2-Ant adducts. TS1: Cl-NO_2-Ant→nitro-Ant+HCl, TS2: Cl-NO_2-Ant+H_2O→nitro-Ant+HCl+H_2O, TS3: Cl-NO_2-Ant+$2H_2O$→nitro-Ant+HCl+$2H_2O$. Resonance structures of the Cl-Ant adduct. The material is available free of charge via the Internet at http://www.elsevier.com/.

References

1. F. Chen, W. Hu, Q. Zhong, Atmos. Res. 2013, 124, 53-60.
2. S. Christie, D. Raper, D. S. Lee, P. I. Williams, L. Rye, S. Blakey, C. W. Wilson, P. Lobo, D. Hagen, P. D. Whitefield, Environ. Sci. Technol. 2012, 46, 6393-6400.
3. J. H. Seinfeld, S. N. Pandis, 2006. Atmospheric Chemistry and Physics; Wiley-Interscience: New York, ISBN 9471720186.
4. A. Bozlaker, A. Muezzinoglu, M. Odabasi, J. Hazard. Mater. 2008, 153, 1093-1102.
5. M. Nadal, M. Schuhmacher, J. L. Domingo, Environ. Pollut. 2004, 132, 1-11.
6. J. W. Li, X. Shang, Z. X. Zhao, R. L. Tanguay, Q. X. Dong, C. J. Huang, J. Hazard. Mater. 2010, 173, 75-81.
7. T. T. T. Dong, B. K. Lee, Chemosphere, 2009, 74(9), 1245-1253.
8. H. Z. Shen, Y. Huang, R. Wang, D. Zhu, W. Li, G. F. Shen, B. Wang, Y. Y. Zhang, Y. C. Chen, Y. Lu, H. Chen, T. C. Li, K. Sun, B. G. Li, W. X. Liu, J. F. Liu, S. Tao, Environ. Sci. Technol. 2013, 47, 6415-6424.
9. C. E. Boström, P. Gerde, A. Hanberg, B. Jernström, C. Johansson, T. Kyrklund, A. Rannug, M. Törnqvist, K. Victorin, R. Westerholm, Environ. Health Perspect. 2002, 110, 451-488.
10. W. L. Xue, D. Warshawsky, Toxicol. Appl. Pharmacol. 2004, 206, 73-93.
11. N. Ramírez, A. Cuadras, E. Rovira, R. M. Marcé, F. Borrull, Environ. Health Perspect. 2011, 119, 1110-1116.
12. I. J. Keyte, R. M. Harrison, G. Lammel, Chem. Soc. Rev. 2013, 42, 9333-9391.

13. L. Wang, J. Arey, R. Atkinson, Environ. Sci. Technol. 2005, 39, 5302-5310.

14. B. Praña, R. Gomperts, J. A. Sordo, Chem. Phys. Lett. 2004, 392, 236-241.

15. A. K. Croft, H. M. Howard-Jones, C. E. Skates, C. C. Wood, Org. Biomol. Chem., 2011, 9, 7439-7447.

16. A. Saiz-Lopez, R. V. Glasow, Chem. Soc. Rev. 2012, 41, 6448-6472.

17. P. S. Monks, Chem. Soc. Rev. 2005, 34, 376-395.

18. K. Kakimoto, H. Nagayoshi, Y. Konishi, K. Kajimura, T. Ohura, K. Hayakawa, A. Toriba, Chemosphere 2014, 111, 40-46.

19. A. Kitazawa, T. Amagai, T. Ohura, Environ. Sci. Technol. 2006, 40 (15), 4592-4598.

20. K. Sankoda, K. Nomiyama, T. Yonehara, T. Kuribayashi, R. Shinohara, Chemosphere, 2012, 88 (5), 542-547.

21. X. X. Long, J. F. Niu, Chemosphere, 2007, 67 (10), 2028-2034.

22. M. Riva, R. M. Healy, P. M. Flaud, E. Perraudin, J. C. Wenger, E. Villenave, 2015, J. Phys. Chem. A, 119(45), 11170-11181.

23. K. F. Ho, S. S. H. Ho, S. C. Lee, Y. Cheng, J. C. Chow, J. G. Watson, P. K. K. Louie, L.W. Tian, Atmos. Environ. 2009, 43, 6343-6351.

24. W. L. Ma, Y. F. Li, H. Qi, D. Z. Sun, L. Y. Liu, D. G. Wang, Chemosphere, 2010, 79(4), 441-447.

25. K. Slezakova, D. Castro, A. Begonha, C. Delerue-Matos, M. Alvim-Ferraz, S. Morais, M. Pereira, Microchem. J. 2011, 99, 51-59.

26. G. P. Robert, Density functional theory. Annu. Rev. Phys. Chem. 1983, 34,

631-656.

27. M. Frisch, G. Trucks, H. B. Schlegel, G. Scuseria, M. Robb, J. Cheeseman, G. Scalmani, V. Barone, B. Mennucci, G. Petersson, 2009. Gaussian 09, revision A. 02; Gaussian. Inc., Wallingford, CT 270, 271.

28. D. R. Glowacki, C. H. Liang, C. Morley, M. J. Pilling, S. H. Robertson, J. Phys. Chem. A 2012, 116, 9545-9560.

29. L. Vereecken, J. S. Francisco, Chem. Soc. Rev. 2012, 41, 6259-6293.

30. O. Sokolov, M. D. Hurley, T. J. Wallington, E. W. Kaiser, J. Platz, O. J. Nielsen, F. Berho, M.-T. Rayez, R. Lesclaux, J. Phys. Chem. A 1998, 102(52), 10671-10681.

31. D. L. Wang, X. B. Xu, S. G. Chu, D. R. Zhang, Chemosphere, 2003, 53 (5), 495-503.

32. T. Ohura, Sci. World J. 2007, 7, 372-380.

33. V. Vaida, J. D. Simon, Science 1995, 268, 1443-1448.

34. K. Pfeilsticker, A. Lotter, C. Peters, H. Bösch, Science 2003, 300, 2078-2080.

35. Q. Z. Zhang, R. Gao, F. Xu, Q. Zhou, G.B. Jiang, T. Wang, J.M. Chen, J.T. Hu, W. Jiang, W. X. Wang, Environ. Sci. Technol. 2014, 48(9), 5051-5057.

36. J. Zhou, J. W. Chen, C-H. Liang, Q. Xie, Y-N. Wang, S.Y. Zhang, X. L. Qiao, X. H. Li, Environ. Sci. Technol. 2011, 45, 4839-4845.

37. C. B. Faxon, D. T. Allen, Environ. Chem. 2013, 10, 221-233.

Table 1. Calculated rate constants (cm^3 molecule^{-1} s^{-1}) for the crucial elementary reactions involved in the Cl-initiated oxidation of Ant and Pyr at 298 K and 1 atm.

Reactions	Rate constants
Ant +Cl→Cl-Ant adducts	(k_a) 5.87×10^{-12}
Ant +Cl→IM1	(k_1) 1.01×10^{-13}
Ant+Cl→IM2	(k_2) 8.69×10^{-13}
Ant+Cl→IM3	(k_3) 9.93×10^{-13}
Pyr+Cl→Cl-Pyr adducts	(k_p) 2.81×10^{-12}
Pyr+Cl→IM4	(k_4) 5.06×10^{-13}
Pyr+Cl→IM5	(k_5) 1.97×10^{-13}

Figure Captions

Figure 1. The Cl addition reaction scheme of Ant and Pyr embedded with the potential barrier Δ*E* (kcal/mol) and reaction heat Δ*H* (kcal/mol). Δ*H* is calculated at 0 K.

Figure 2. The formation scheme of chloro-Ants and chloro-Pyrs embedded with the potential barrier Δ*E* (kcal/mol) and reaction heat Δ*H* (kcal/mol). Δ*H* is calculated at 0 K.

Figure 3. The O_2/NO addition reaction scheme of Cl-Ant and Cl-Pyr adducts embedded with the potential barrier Δ*E* (kcal/mol) and reaction heat Δ*H* (kcal/mol).

Figure 4. The reaction scheme of intramolecular H shift of O_2-Cl-Ant and O_2-Cl-Pyr adducts embedded with the potential barrier Δ*E* (kcal/mol) and reaction heat Δ*H* (kcal/mol).

Figure 5. The reaction scheme of the cyclization of O_2-Cl-Ant and O_2-Cl-Pyr embedded with the potential barrier Δ*E* (kcal/mol) and reaction heat Δ*H* (kcal/mol) in the presence of O_2 and NO. Δ*H* is calculated at 0 K.

Figure 6. The formation scheme of nitro-Ants and nitro-Pyrs embedded with the potential barrier Δ*E* (kcal/mol) and reaction heat Δ*H* (kcal/mol). Δ*H* is calculated at 0 K.

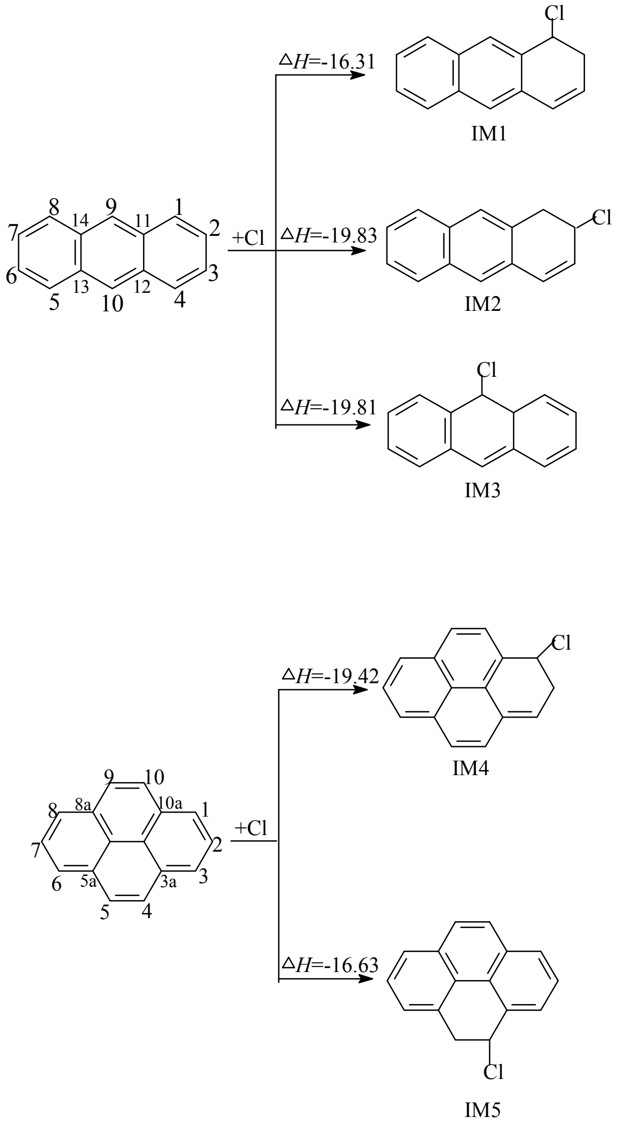
8
9
1
7
14
11
2
6
13
12
3
5
10
4
+Cl
△H=-16.31
Cl
IM1
△H=-19.83
Cl
IM2
△H=-19.81
Cl
IM3
△H=-19.42
Cl
IM4
9
10
8
8a
10a
1
7
2
6
5a
3a
3
5
4
+Cl
△H=-16.63
Cl
IM5

Figure 1

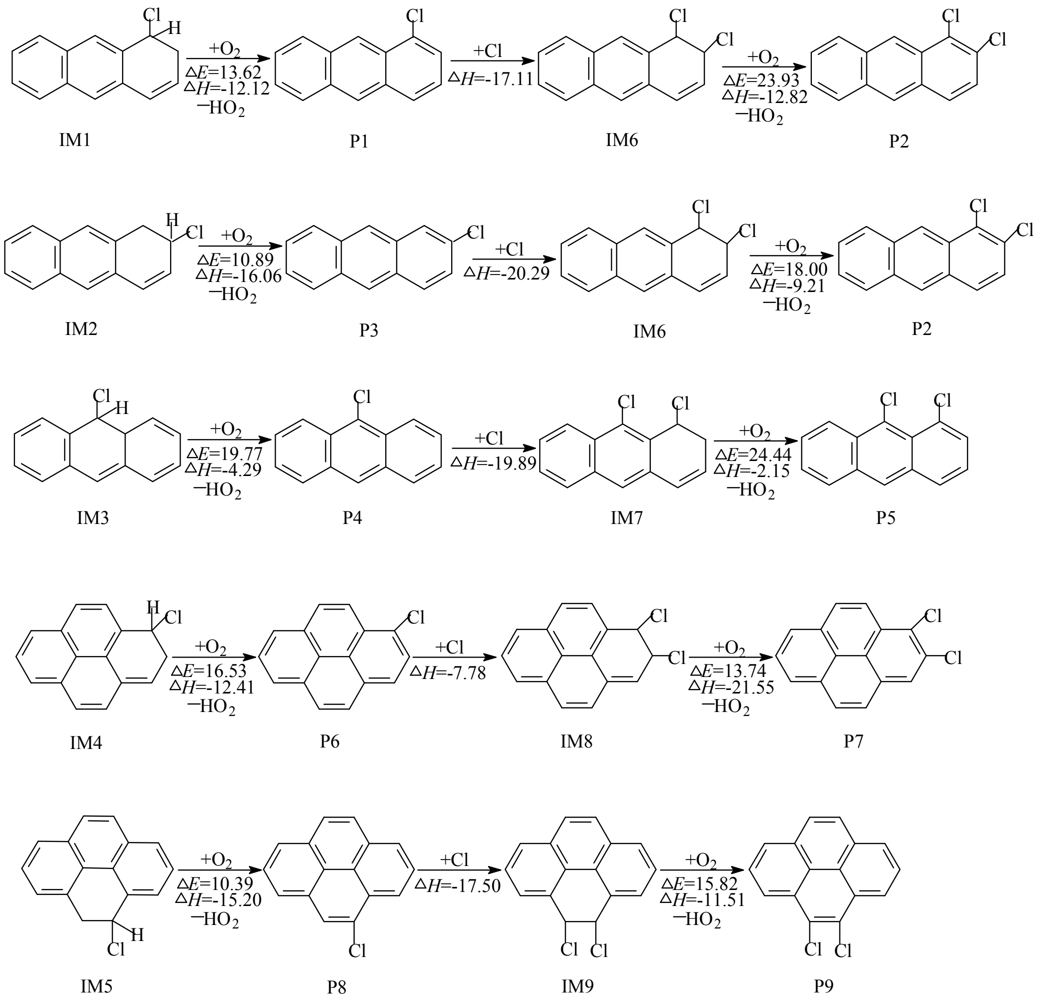
Cl
H
+O2
△E=13.62
△H=-12.12
−HO2
IM1
Cl
P1
+Cl
△H=-17.11
Cl
Cl
IM6
+O2
△E=23.93
△H=-12.82
−HO2
Cl
Cl
P2
H
Cl
+O2
△E=10.89
△H=-16.06
−HO2
IM2
Cl
P3
+Cl
△H=-20.29
Cl
Cl
IM6
+O2
△E=18.00
△H=-9.21
−HO2
Cl
Cl
P2
Cl
H
+O2
△E=19.77
△H=-4.29
−HO2
IM3
Cl
P4
+Cl
△H=-19.89
Cl
Cl
IM7
+O2
△E=24.44
△H=-2.15
−HO2
Cl
Cl
P5
H
Cl
+O2
△E=16.53
△H=-12.41
−HO2
IM4
Cl
P6
+Cl
△H=-7.78
Cl
Cl
IM8
+O2
△E=13.74
△H=-21.55
−HO2
Cl
Cl
P7
Cl
H
+O2
△E=10.39
△H=-15.20
−HO2
IM5
Cl
P8
+Cl
△H=-17.50
Cl
Cl
IM9
+O2
△E=15.82
△H=-11.51
−HO2
Cl
Cl
P9

Figure 2

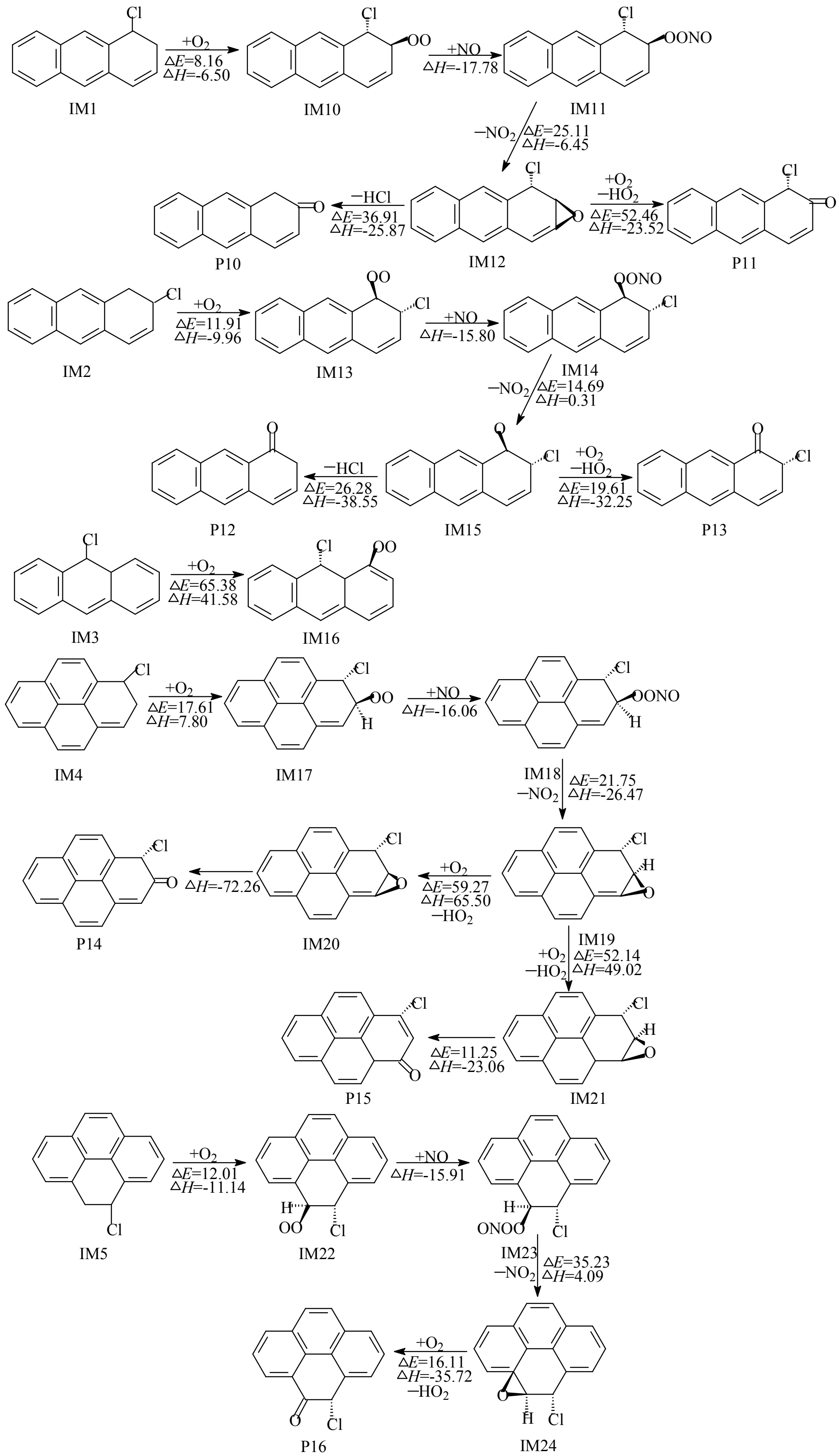
Cl
+O2
ΔE=8.16
ΔH=-6.50
IM1
Cl
OO
IM10
+NO
ΔH=-17.78
Cl
OONO
IM11
−NO2
ΔE=25.11
ΔH=-6.45
Cl
O
IM12
−HCl
ΔE=36.91
ΔH=-25.87
O
P10
+O2
−HO2
ΔE=52.46
ΔH=-23.52
Cl
O
P11
Cl
IM2
+O2
ΔE=11.91
ΔH=-9.96
OO
Cl
IM13
+NO
ΔH=-15.80
OONO
Cl
IM14
−NO2
ΔE=14.69
ΔH=0.31
O
Cl
IM15
−HCl
ΔE=26.28
ΔH=-38.55
O
P12
+O2
−HO2
ΔE=19.61
ΔH=-32.25
O
Cl
P13
Cl
IM3
+O2
ΔE=65.38
ΔH=41.58
Cl
OO
IM16
Cl
IM4
+O2
ΔE=17.61
ΔH=7.80
Cl
OO
H
IM17
+NO
ΔH=-16.06
Cl
OONO
H
IM18
−NO2
ΔE=21.75
ΔH=-26.47
Cl
H
O
+O2
ΔE=59.27
ΔH=65.50
−HO2
Cl
O
IM20
ΔH=-72.26
Cl
O
P14
IM19
+O2
−HO2
ΔE=52.14
ΔH=49.02
Cl
H
O
IM21
ΔE=11.25
ΔH=-23.06
Cl
O
P15
Cl
IM5
+O2
ΔE=12.01
ΔH=-11.14
H
OO
Cl
IM22
+NO
ΔH=-15.91
H
ONOO
Cl
IM23
−NO2
ΔE=35.23
ΔH=4.09
O
H
Cl
IM24
+O2
ΔE=16.11
ΔH=-35.72
−HO2
O
Cl
P16

Figure 3

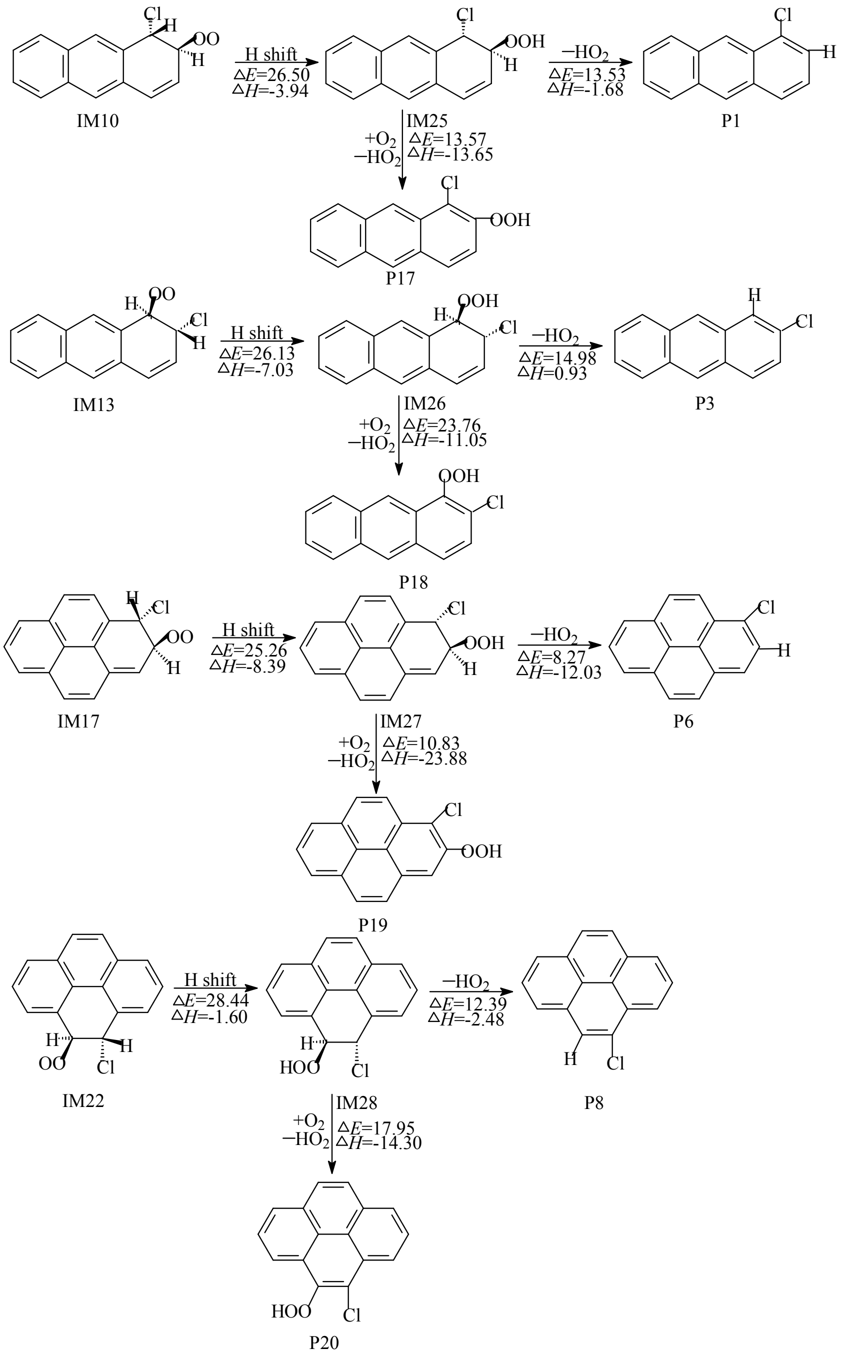
IM10
H shift
ΔE=26.50
ΔH=-3.94
IM25
−HO2
ΔE=13.53
ΔH=-1.68
P1
+O2
−HO2
ΔE=13.57
ΔH=-13.65
P17
IM13
H shift
ΔE=26.13
ΔH=-7.03
IM26
−HO2
ΔE=14.98
ΔH=0.93
P3
+O2
−HO2
ΔE=23.76
ΔH=-11.05
P18
IM17
H shift
ΔE=25.26
ΔH=-8.39
IM27
−HO2
ΔE=8.27
ΔH=-12.03
P6
+O2
−HO2
ΔE=10.83
ΔH=-23.88
P19
IM22
H shift
ΔE=28.44
ΔH=-1.60
IM28
−HO2
ΔE=12.39
ΔH=-2.48
P8
+O2
−HO2
ΔE=17.95
ΔH=-14.30
P20
Cl
H
OO
OOH
HOO

Figure 4

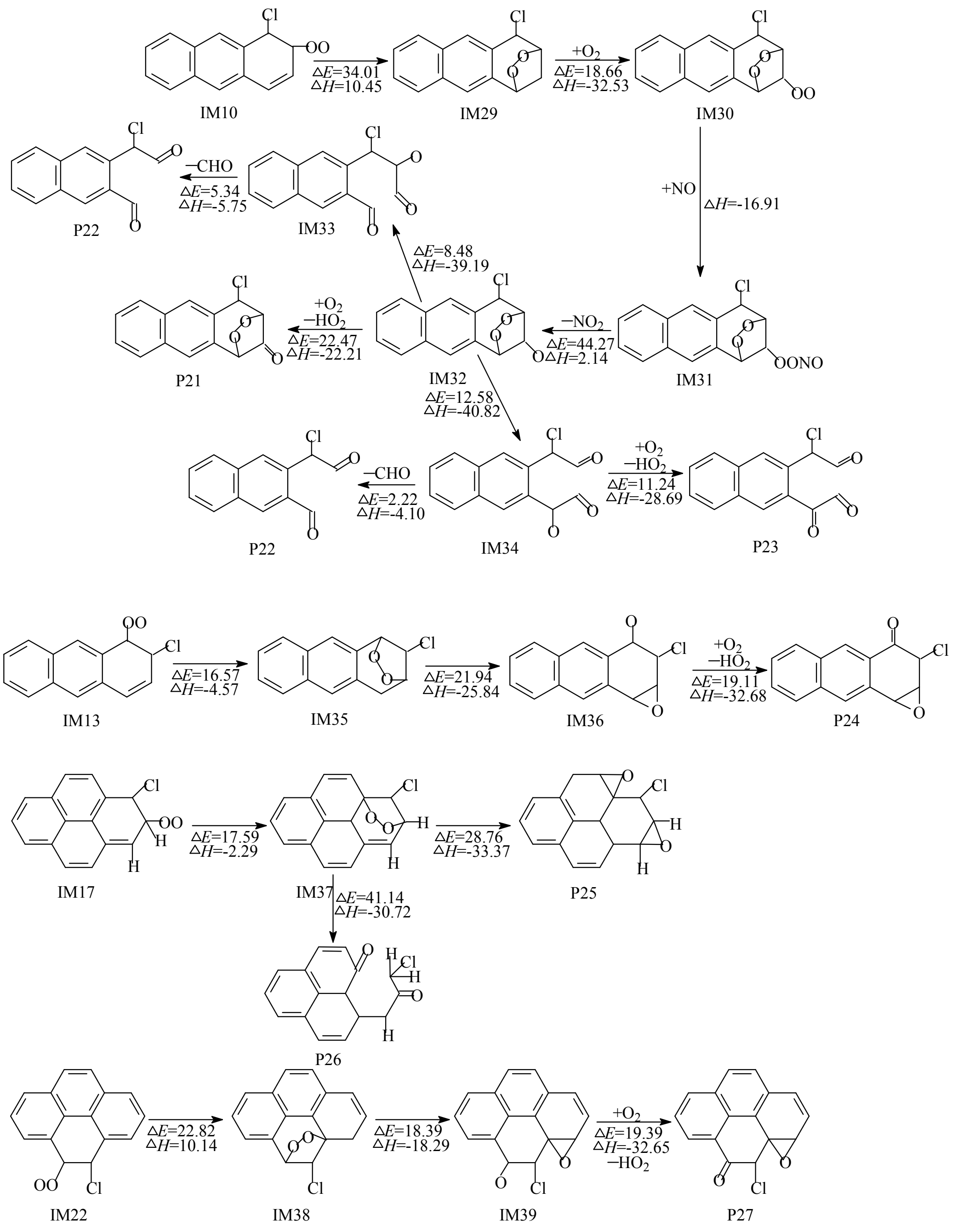
Cl
OO
ΔE=34.01
ΔH=10.45
IM10
Cl
O
O
IM29
+O2
ΔE=18.66
ΔH=-32.53
Cl
O
O
OO
IM30
+NO
ΔH=-16.91
Cl
O
O
OONO
IM31
−NO2
ΔE=44.27
ΔH=2.14
Cl
O
O
O
IM32
ΔE=8.48
ΔH=-39.19
Cl
O
O
O
IM33
−CHO
ΔE=5.34
ΔH=-5.75
Cl
O
O
P22
+O2
−HO2
ΔE=22.47
ΔH=-22.21
Cl
O
O
O
P21
ΔE=12.58
ΔH=-40.82
Cl
O
O
O
IM34
−CHO
ΔE=2.22
ΔH=-4.10
Cl
O
O
P22
+O2
−HO2
ΔE=11.24
ΔH=-28.69
Cl
O
O
O
P23
OO
Cl
IM13
ΔE=16.57
ΔH=-4.57
O
O
Cl
IM35
ΔE=21.94
ΔH=-25.84
O
Cl
O
IM36
+O2
−HO2
ΔE=19.11
ΔH=-32.68
O
Cl
O
P24
Cl
OO
H
H
IM17
ΔE=17.59
ΔH=-2.29
Cl
O
O
H
H
IM37
ΔE=28.76
ΔH=-33.37
O
Cl
H
O
H
P25
ΔE=41.14
ΔH=-30.72
O
H
Cl
H
O
H
P26
OO
Cl
IM22
ΔE=22.82
ΔH=10.14
O
O
Cl
IM38
ΔE=18.39
ΔH=-18.29
O
O
Cl
IM39
+O2
ΔE=19.39
ΔH=-32.65
−HO2
O
O
Cl
P27

Figure 5

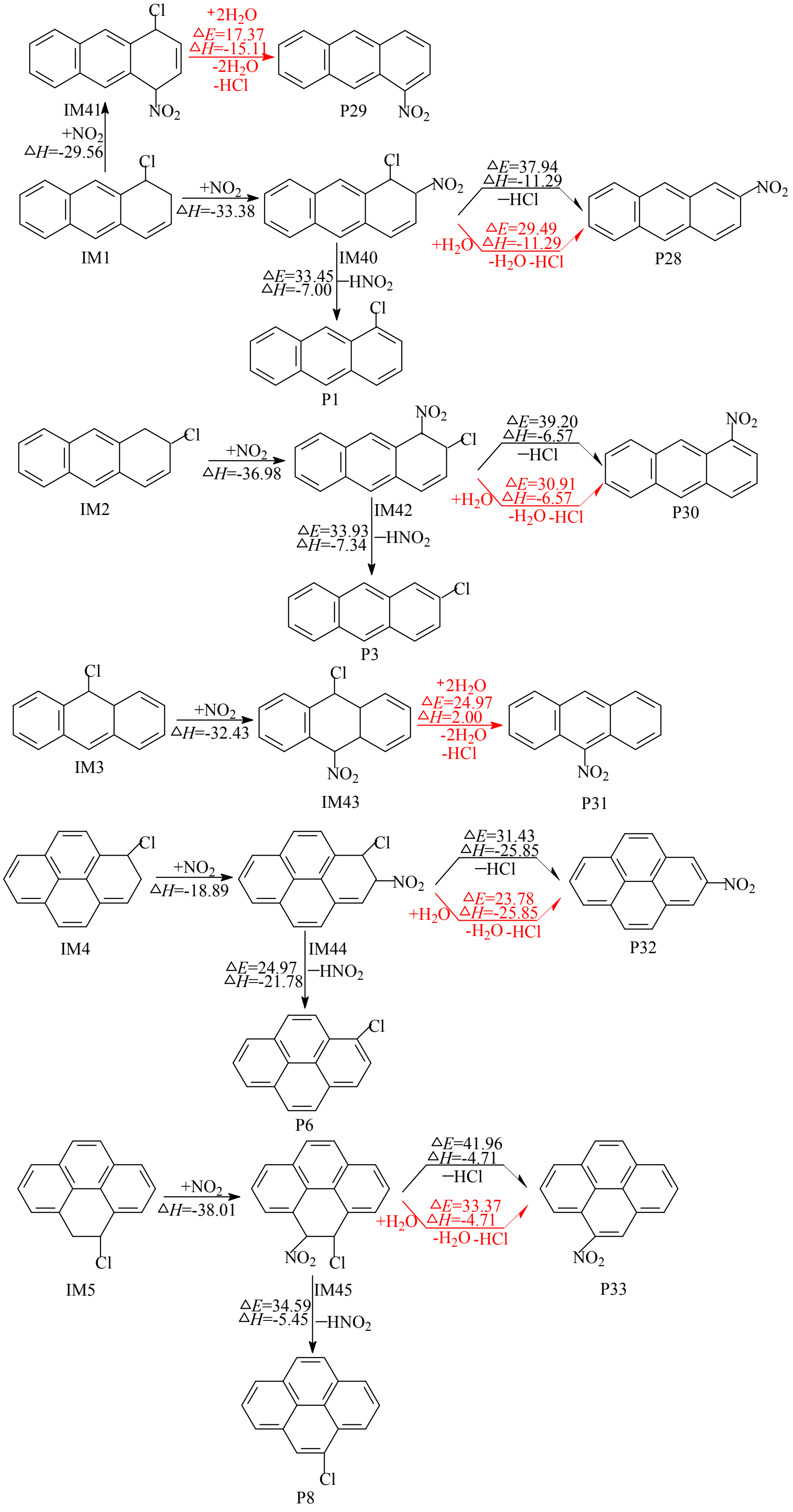
Cl
+2H$_2$O
ΔE=17.37
ΔH=-15.11
-2H$_2$O
-HCl
IM41
NO$_2$
P29
NO$_2$
+NO$_2$
ΔH=-29.56
Cl
+NO$_2$
ΔH=-33.38
IM1
Cl
NO$_2$
ΔE=37.94
ΔH=-11.29
−HCl
+H$_2$O
ΔE=29.49
ΔH=-11.29
-H$_2$O -HCl
NO$_2$
P28
IM40
ΔE=33.45
ΔH=-7.00
−HNO$_2$
Cl
P1
Cl
IM2
+NO$_2$
ΔH=-36.98
NO$_2$
Cl
ΔE=39.20
ΔH=-6.57
−HCl
+H$_2$O
ΔE=30.91
ΔH=-6.57
-H$_2$O -HCl
NO$_2$
P30
IM42
ΔE=33.93
ΔH=-7.34
−HNO$_2$
Cl
P3
Cl
IM3
+NO$_2$
ΔH=-32.43
Cl
NO$_2$
IM43
+2H$_2$O
ΔE=24.97
ΔH=2.00
-2H$_2$O
-HCl
NO$_2$
P31
Cl
IM4
+NO$_2$
ΔH=-18.89
Cl
NO$_2$
ΔE=31.43
ΔH=-25.85
−HCl
+H$_2$O
ΔE=23.78
ΔH=-25.85
-H$_2$O -HCl
NO$_2$
P32
IM44
ΔE=24.97
ΔH=-21.78
−HNO$_2$
Cl
P6
Cl
IM5
+NO$_2$
ΔH=-38.01
NO$_2$
Cl
ΔE=41.96
ΔH=-4.71
−HCl
+H$_2$O
ΔE=33.37
ΔH=-4.71
-H$_2$O -HCl
NO$_2$
P33
IM45
ΔE=34.59
ΔH=-5.45
−HNO$_2$
Cl
P8

Figure 6